A Platinum Open Access Journal for Organic Chemistry

Review

Free to Authors and Readers | DOAJ Seal | *Arkivoc* **2026** (2) 202612560

Developing new accesses to silylated and germylated heterocycles: An overview

Jacques Maddaluno[a,b] and Muriel Durandetti[a]*

[a]Univ Rouen Normandie, INSA Rouen Normandie, Univ Caen Normandie, ENSICAEN, CNRS, CARMeN UMR 6064, F-76000 Rouen, France

[b]Sorbonne Université, CNRS, Laboratoire d'Archéologie Moléculaire et Structurale UMR 8220, F-75005 Paris, France

Email: muriel.durandetti@univ-rouen.fr

Received 02-09-2026 **Accepted** 04-12-2026 **Published on line** 04-19-2026

Abstract

Finding new approaches to heterocycles is an ongoing challenge in synthetic organic chemistry, as these structures are present in many molecules of major interest, particularly those developed for applications in medicinal chemistry. The carbon, silicon and germanium atoms exhibit similar structural features, such as valence and geometry, which explains why substituting one of these chemical elements for another ensures isosteric relationships between the corresponding derivatives. Consequently, the synthesis of new silylated and germylated heterocycles, through both inter- and intramolecular pathways, has attracted great attention in recent years. This account reviews the methods we have developed in our group to access such structures.

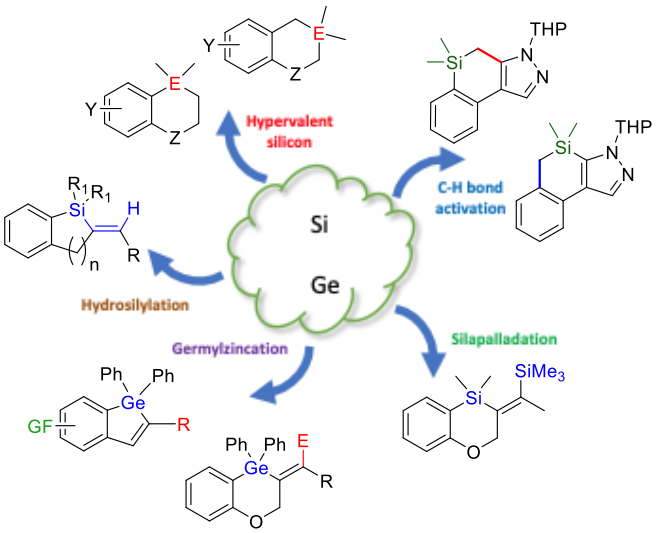

Keywords: Cyclization, germanium, heterocycles, silicon, Si–C bond.

Table of Contents

1. Introduction

Silicon was first isolated by Jöns Jacob Berzelius in 1824 as an amorphous solid.[1] As a metalloid with atomic number 14, it is the second most abundant element in the Earth's crust (25.7%), following oxygen (46.4%). However, silicon does not occur in its pure form in nature, but predominantly as oxides such as silica or quartz. Carbon, silicon, and germanium, which belong to the same column of the periodic table, enforce structural similarities in the molecules in which they are incorporated, particularly in terms of valence and geometry. Nevertheless, they differ in certain physical and chemical properties, including covalent radius and electronegativity. The incorporation of silicon or germanium into organic compounds enables modulation of their chemical and physicochemical properties, a feature that is particularly valuable in medicinal chemistry.[2-5] For instance, organosilylated compounds offer several advantages for medical applications, such as increased lipophilicity, enhanced acidity, and access to alternative metabolic pathways, providing distinct benefits over purely carbon-based analogues in certain cases.[6-7] Beyond medicinal chemistry, carbon-silicon/germanium isostery also plays a key role in materials science,[8-10] where organosilylated and germylated compounds have emerged as promising candidates for tuning material properties, notably in luminescence and, more specifically, fluorescence.[11] Over the past few decades, synthetic chemists have explored the consequences of replacing carbon with silicon or germanium on the physicochemical properties of target compounds[12] and, in the case of bioactive molecules, on their biological activity.[13] To advance this field further, the design of new families of Si- and Ge-containing molecules is essential, requiring the development of efficient synthetic methodology for C–Si and C–Ge bond formation. In this context, our group has focused on creating novel strategies for the synthesis of silylated and germylated compounds. In this account, we will highlight our contributions to this area.

2. Synthetic Approaches to Silylated and Germylated Heterocycles

2.1. Synthesis of silylated and germylated heterocycles *via* anionic rearrangements involving hypervalent silicon and germanium

The first method developed for C–Si bond formation, and still one of the most widely employed today, relies on a straightforward nucleophilic substitution of a leaving group attached to a silicon atom. The efficiency of this transformation is favored by the pronounced electropositivity of silicon compared to carbon (C: 2.55 vs. Si: 1.9 on the Pauling scale). As early as the 1950s, Hitchcock applied this strategy in the synthesis of diphenylphenoxasilines.[14] The approach involves a double bromine-lithium exchange to generate dilithiated intermediates, which, upon reaction with diphenyldichlorosilane, deliver the target compounds with notable electronic properties in yields of 59% and 78%.

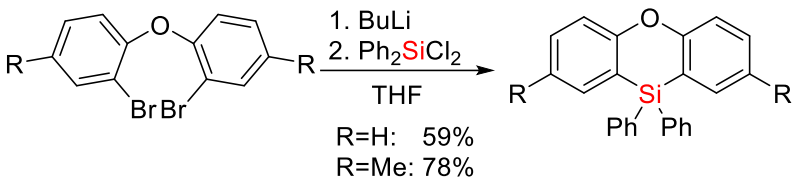

Scheme 1. Diphenylphenoxasilines synthesis.

The lack of general-synthesis procedures prompted us to focus on the preparation of the hydrasilaquinoline **1** and silachroman **2** fragments (Figure 1), previously obtained with moderate yields and limited scope.[15] We decided first to perform the cyclisation by intramolecular nucleophilic substitution.

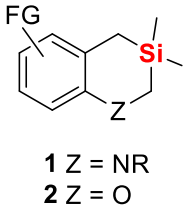

Figure 1. Structures of desired hydrasilaquinoline **1** and silachroman **2**.

O-alkylating-2-iodophenol with dichloromethyldimethylsilane under mild conditions led directly to the silylated substrate **3**. The expected cyclisation was triggered using 1 equivalent of *n*-BuLi in THF, but, to our surprise, the two regioisomers **2a** and **2b** were obtained in 85% yield and in a 60/40 ratio (Scheme 2).[16-17] This result could be rationalized through a common hypervalent silicon intermediate **A**, resulting from a direct attack of the phenyllithium on the silicon nucleus. This latter would then rearrange into one or the other regioisomer.

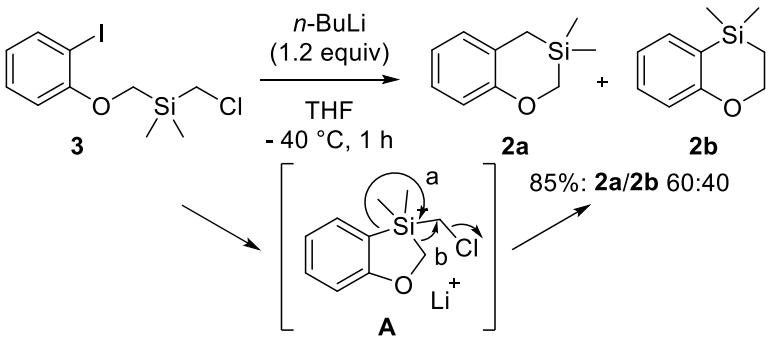

Scheme 2. Anionic access to silachromane **2**.

To support this hypothesis, based on that proposed by Matteson for boron derivatives, we prepared the siladihydrobenzofuran **4**, easily from the same 2-iodophenol and chloromethyldimethylchlorosilane (Scheme 3). Reacting **4** with the carbenoid resulting from the reaction between iodochloromethane and the MeLi.LiBr complex, led directly to a 50/50 mixture of **2a** and **2b**. This result is in good agreement with the formation of the silicon intermediate **A**.

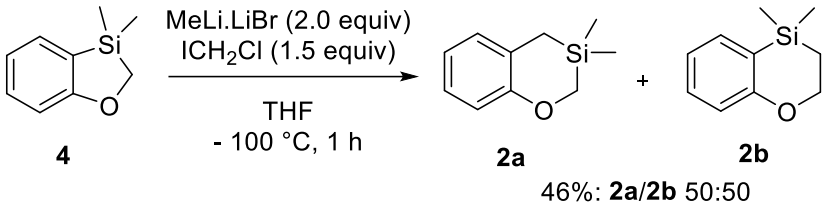

Scheme 3. Indirect evidence of the hypervalent silicon intermediate **A**.

We next decided to extend this methodology to the synthesis of hydrasilaquinoline **1** and prepared the N-Boc tethered intermediate **5** from 2-iodoaniline. In similar conditions, the cyclisation occurred smoothly and afforded the two regioisomers **1a-b** in 84% yields and a 45/55 ratio. When the same process was applied to the silylated derivative of 2-iodothiophenol **6**, the sole 1,4-thiochromane **7a** was isolated in an excellent yield of 99%, without any trace of the 1,3-regioisomer **7b** (Scheme 4). Obviously, the selectivity of the rearrangement of the **A**-type intermediate derived from **6** is influenced by the geometry and the electronic properties associated with sulfur.

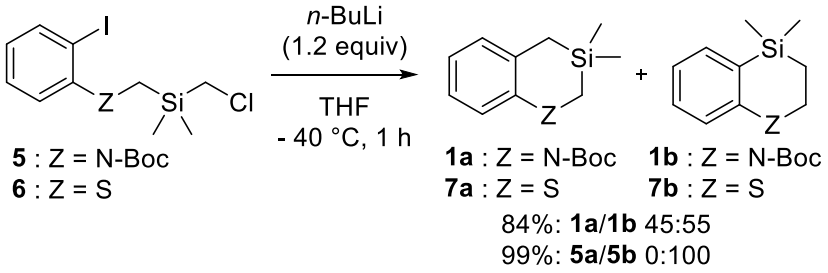

Scheme 4. Extension of the cyclization to aniline and thiophenol derivatives **5** and **6**.

Complementary with, and to better understand the influence of the structure of the aromatic nucleophile on the outcome of this reaction, we prepared a series of substrates derived from variously substituted iodoanilines, since the nitrogenous heterocycles are particularly relevant in medicinal chemistry. If the cyclisation is always observed, and the expected substrates obtained in moderate-to-excellent chemical yields, the regioisomers ratio is strongly dependent on the electronic density of the aromatic substrate. In fact, the logarithm of the **a**/**b** ratio correlates well with the Hammett constants,[18] and the high correlation coefficient (R^2 = 0.94) indicates that the observed trend arises from purely electronic-substituent effects (Figure 2). Overall, electro-donor substituents tend to favor isomer **b**, whereas electron-withdrawing ones give isomer **a** preferentially. Note that this observation is consistent with the hypothesis of a penta-coordinated silicon intermediate, since the Si–C(sp2) bond will be preferentially cleaved when the aromatic ring is electro-enriched.

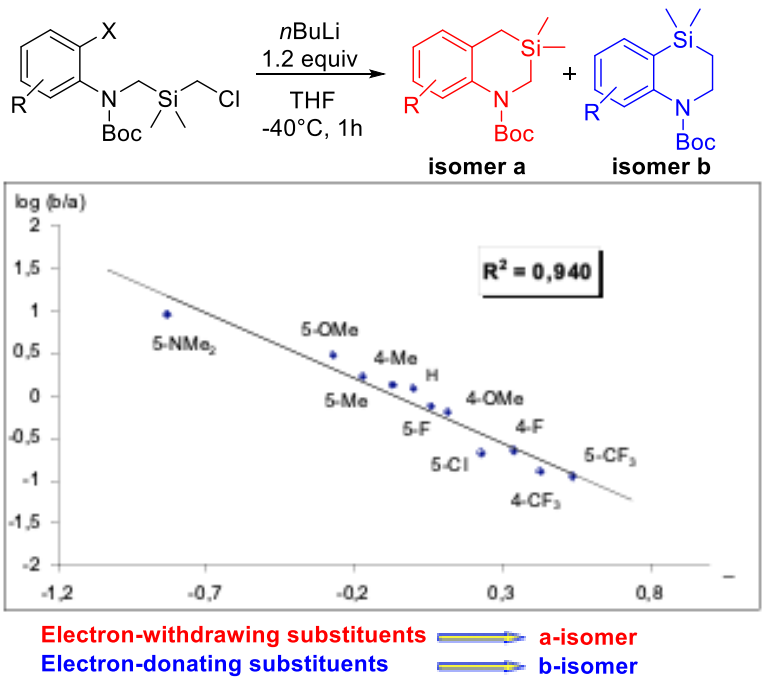

Figure 2. Aromatic substituents effect.

The scope of this reaction seems relatively large (Table 1). It has been applied to a significant selection of aromatic and heteroaromatic substrates, bearing the silicon appendage on O, N or S tethers. If the thiophenic substrates react as a simple phenyl ring, the electron-deficient pyridyl derivatives afford exclusively, and expectedly, isomers **a**. In contrast, complete selectivity in favor of **b** is observed with the S-tether, which can be attributed to a substantial modification of the nucleophilic substitution geometry imposed by the longer C–S bond.

Table 1. Aromatic substituents effect on the ratio **a**/**b**

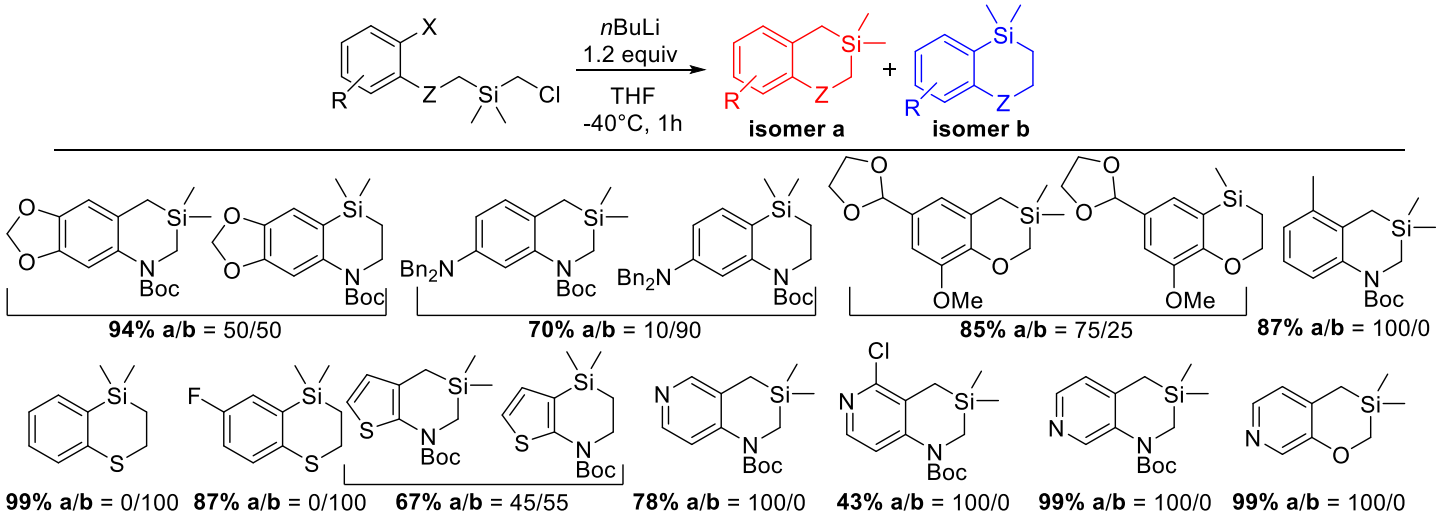

At this stage, it became interesting to evaluate the effect played by silicon substituents R/R' (Scheme 5). Replacing one of the two methyls by a phenyl favors the sila-Matteson product (isomer **b**), which is even obtained exclusively when dealing with the aniline derivative **8**. Further increasing the degree of silicon

substitution (using diphenylsilane) amplifies this effect; however, an additional five-membered-ring isomeric product is also formed. This outcome is most plausibly explained by an alternative rearrangement of the common pentavalent silicon intermediate, triggering phenyl group migration (shown in brackets in Scheme 5), thereby further supporting the proposed sila-Matteson mechanism.

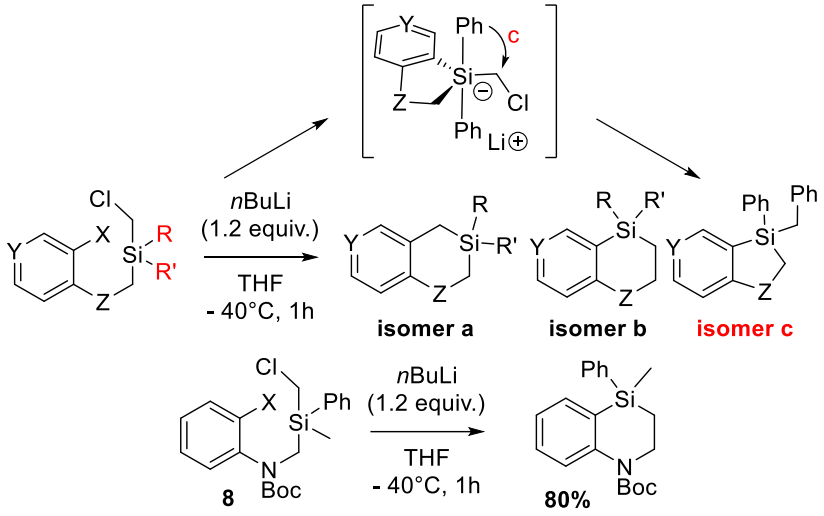

Scheme 5. Effect of the silicon substituents on the selectivity of the cyclization.

We decided then to further extend the process to the synthesis of germylated derivatives. The results indicate that the reaction proceeds via a comparable pentavalent germanium intermediate. A new product, arising from $LiCH_2Cl$ carbenoid elimination (product **d**, Scheme 6), is formed in moderate-to-high yields, depending on the starting material. It even becomes the exclusive outcome when an ortho substituent is present. This behavior likely reflects germanium's larger covalent radius, which hinders intramolecular nucleophilic substitution, and its higher electronegativity, which stabilizes the pentavalent intermediate relative to silicon.

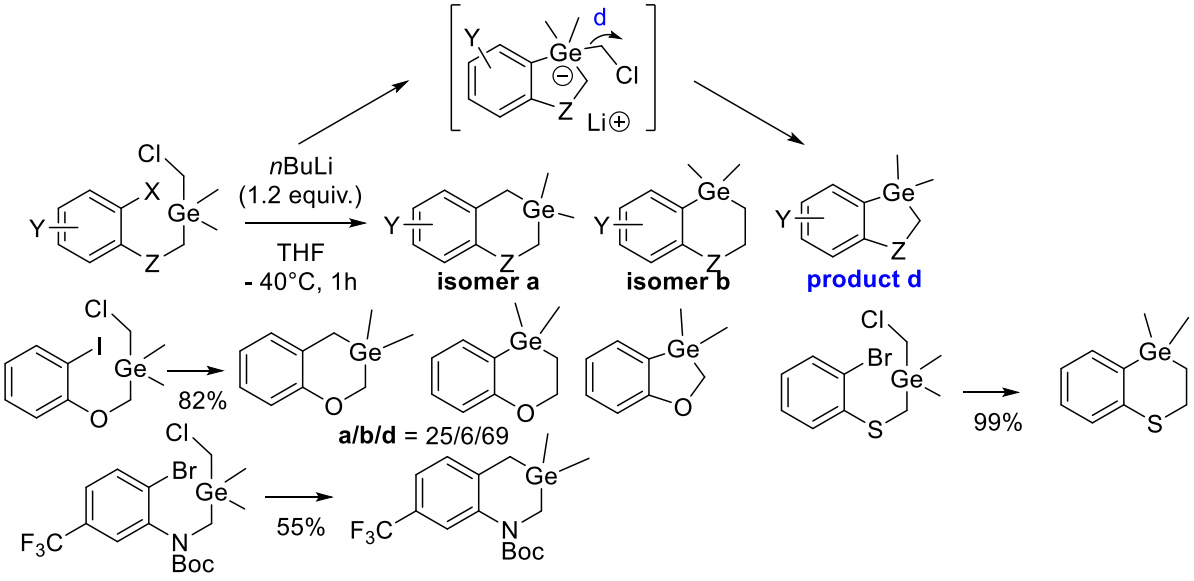

Scheme 6. Extension of the above rearrangement to germylated substrates using *n*- or *t*-BuLi.

In conclusion to this part, we have shown that a sila-Matteson process gives access to four different families of heterocycles in good-to-excellent yields and selectivities that depend on the electronic density on the original aromatic ring, and on the steric hindrance brought by the different substituents. A single product can even be obtained when all parameters converge (Figure 3).

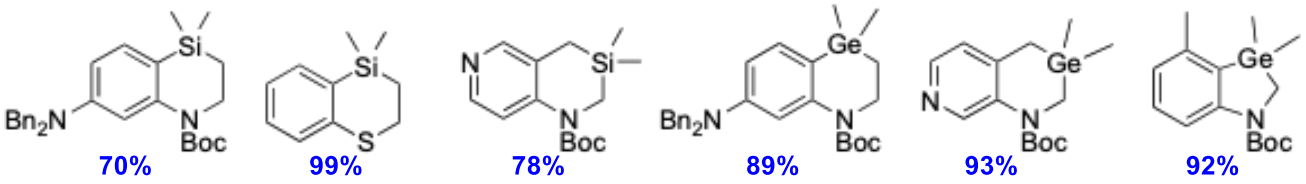

Figure 3. Some examples of high regioselectivies for the synthesis of silylated and germylated scaffolds.

To demonstrate the interest of this chemistry, we tried to apply this methodology to the synthesis of silylated and germylated analogues of Motesanib.[19] This compound is a well-known multi-kinase inhibitor developed by Amgen, later investigated by the Takeda Pharmaceutical Company that reached phase III clinical trials as an anti-angiogenesis candidate.[20] We focused on the eastern part **A** of the molecule, and decided to replace the gem-dimethyl dihydroindole skeleton by an $SiMe_2$-azasiline one (or germylated analogue). It rapidly appeared that aminoazasilines such as those displayed in Figure 3 would be excellent building blocks in a rapid synthesis of these drug candidates (Figure 4).

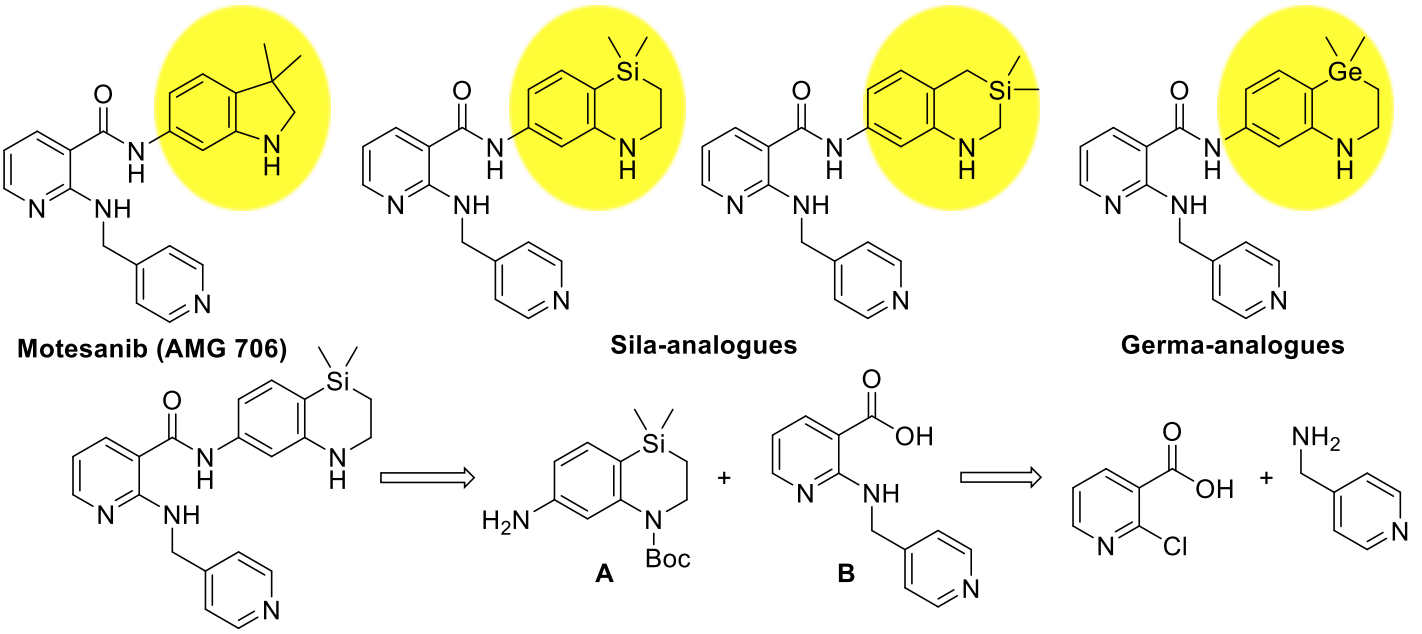

Figure 4. Structure of Motesanib and envisioned derivatives **11a-c**.

The N-dibenzylated substrates **9** and **9'** were easily prepared in 5 classical steps from commercially-available 2-bromo-5-nitroaniline. In the presence of two equivalents of *t*-BuLi, silylated substrate **9** led to the anticipated regio-isomers **b** and **a** in a ratio 90/10, while germylated **9'** led, exclusively, to isomer **b**. Both transformations occurred in very good yields (Scheme 7).

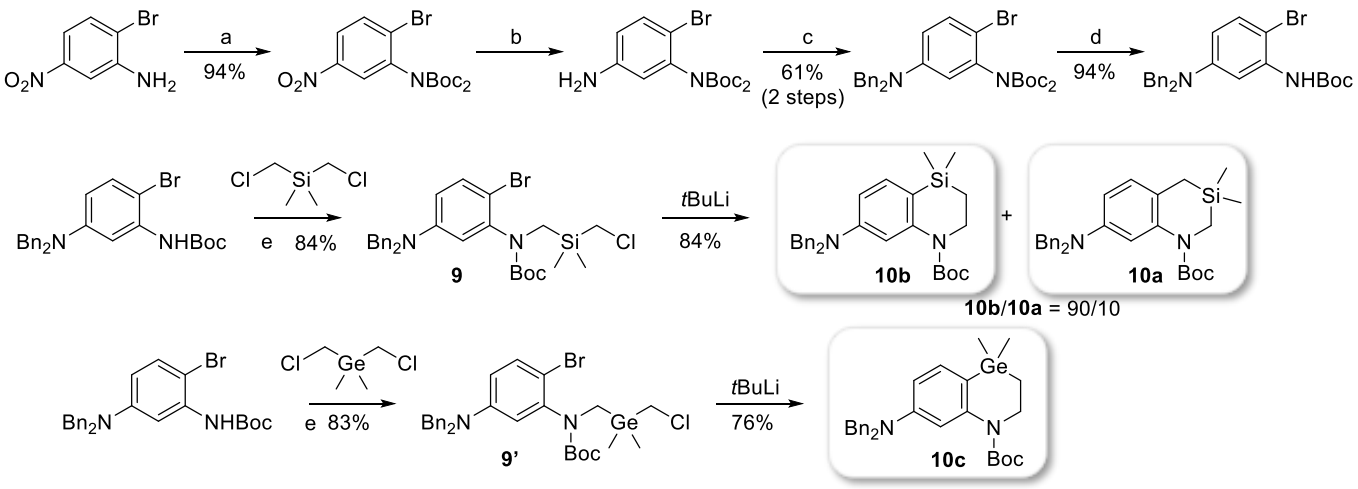

Reagents and conditions: (a) Boc_2O, DMAP, CH_2Cl_2, 24 h, rt; (b) Zn, NH_4Cl, acetone, 4 h, reflux; (c) BnBr, NaI, K_2CO_3, DMF, 24 h, rt; (d) K_2CO_3, MeOH, 4 h, rt; (e) NaH, DMF, 3 h, 80 °C

Scheme 7. Synthesis of building blocks **10a-c**.

The western fragment **B** of Motesanib was synthesized in three steps using a slightly modified scheme compared to that employed by Takeda, as their original route was incompatible with the sensitivity of the azasiline moiety. The challenging amination of the intermediate 2-chloro-3-methylcarboxylate pyridine was carried out under microwave irradiation. The sensitivity of free aminoazasilines **10a-c** necessitated performing a double debenzylation immediately prior to coupling with fragment **B**, with hydrogenolysis proving highly effective for this purpose. Peptide-coupling conditions led to the expected amides **11a-b** in 60-65% yields for the sila-Motesanib precursors, but only 22% for their germanium analogue **11c** (Scheme 8).

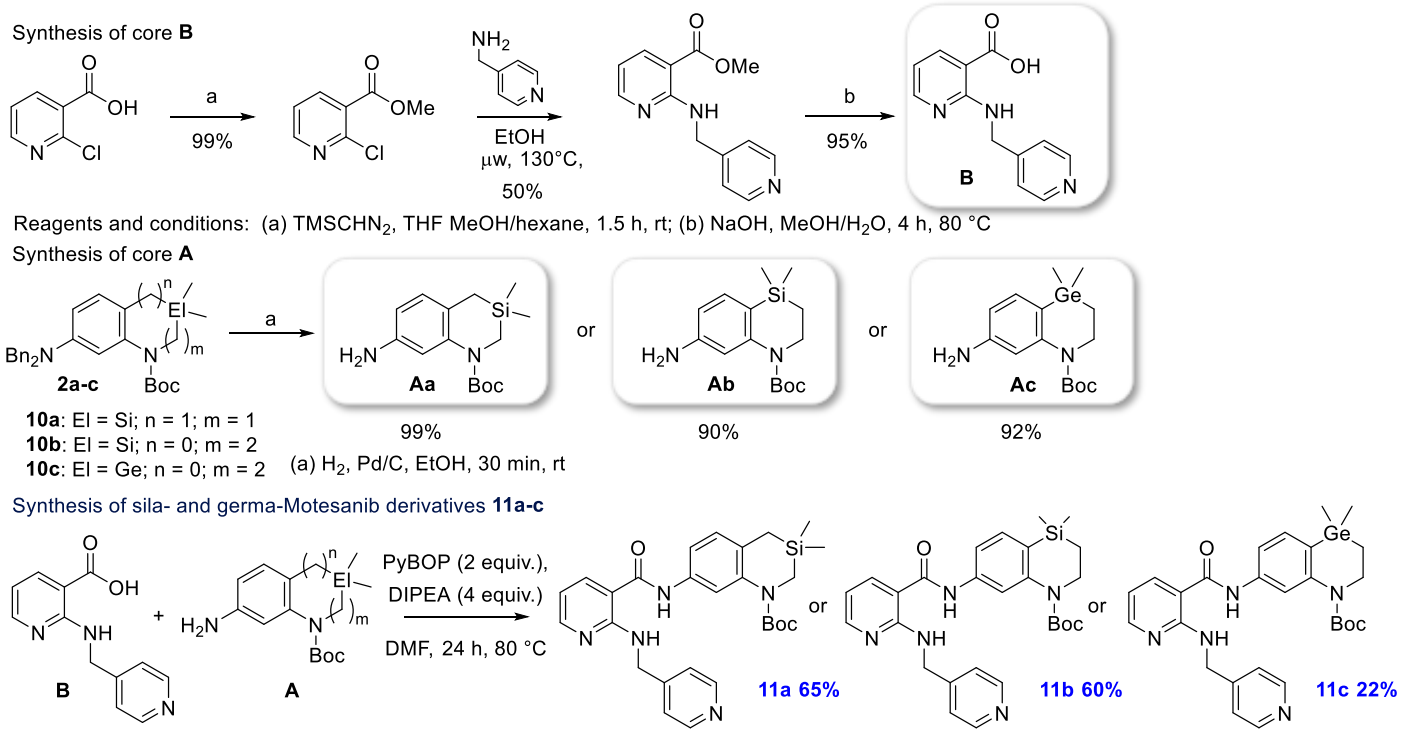

Scheme 8. Synthesis of sila- and germa-Motesanib derivatives **11a-c**.

2.2. Synthesis of silylated pyrazole derivatives by C–H activation of a TMS group

Building on our previous approach to pharmacologically-active molecules, we explored the synthesis of silylated analogues of compounds containing a pyrazole ring. This heterocycle is a key pharmacophore in medicinal chemistry, present in a wide range of biologically-active compounds. In particular, the dihydronaphthopyrazole scaffold emerged as an attractive target, as it has demonstrated antimicrobial, anti-inflammatory, and kinase-inhibiting activities in various drug candidates. We chose to access these structures by a Pd-catalyzed C–H activation of a TMS group, following the pioneering work of Xi and colleagues.[22] To this end, a suitable substrate was synthetized from pyrazole in four steps. A THP-protecting group was retained to exploit its ortho-directing capacity, enabling the selective introduction of the TMS group selectively at the 5 position after deprotonation with *n*-BuLi, achieving an overall yield of 94%.[23] After electrophilic iodination and Suzuki cross-coupling, the resulting biaryl product was obtained in good yields. With this substrate in hands, we attempted the cyclization via intramolecular C–H activation through Pd(0) insertion into the C–Br bond. Unfortunately, all attempts under conventional conditions failed, and the only product obtained was the desilylated compound **14** (Scheme 9).

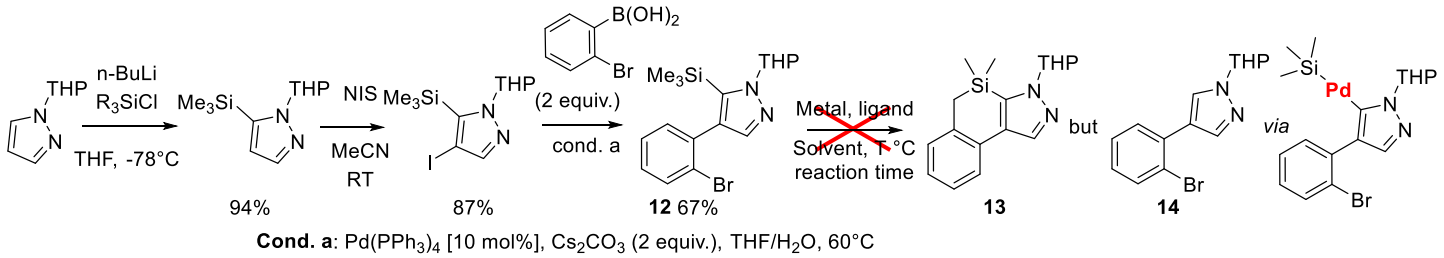

Scheme 9. Synthesis and reactivity of substrate **12**.

To facilitate C–X activation, we attempted to replace the bromine atom with iodine. However, treatment of **12** with *t*-BuLi followed by the addition of I_2, led to the isolation, in good yields, of compound **16**, an isomer of the expected aryliodide **15**. This outcome can be rationalized by a bromine-lithium exchange, followed by intramolecular addition onto the Si atom, and subsequent rearrangement of the resulting hypervalent silicon intermediate (Scheme 10).

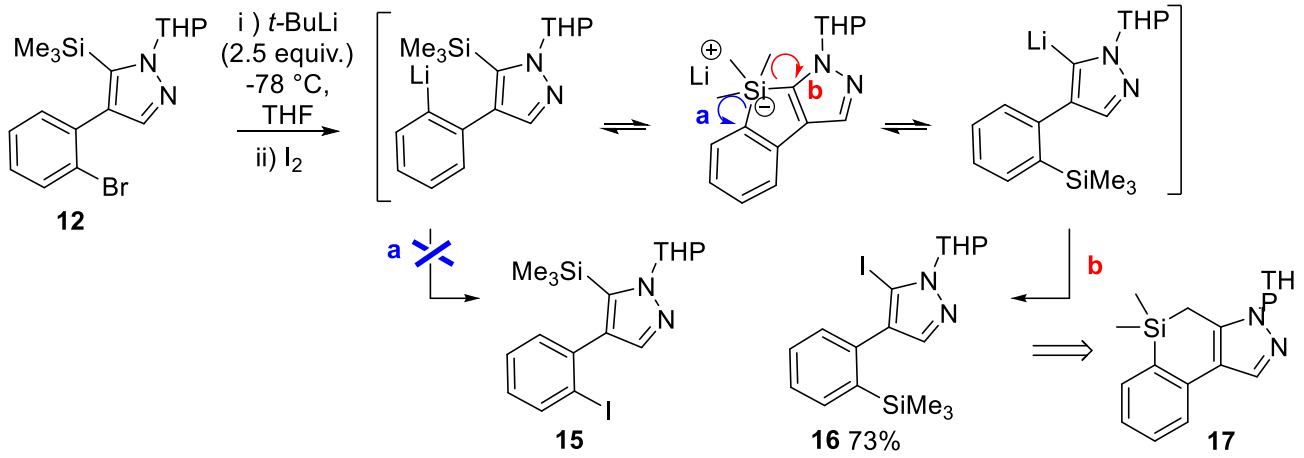

Scheme 10. Reactivity of substrate **12** upon lithium-halogen exchange.

This difficulty was circumvented by converting compound **12** into the corresponding arylzinc,[24-25] which reacted efficiently with I_2 to afford the desired aryliodide **15** (Scheme 11). Overall, this strategy provided access to two isomeric substrates, **13** and **17**, as a result of the unexpected transposition of the silicon atom.

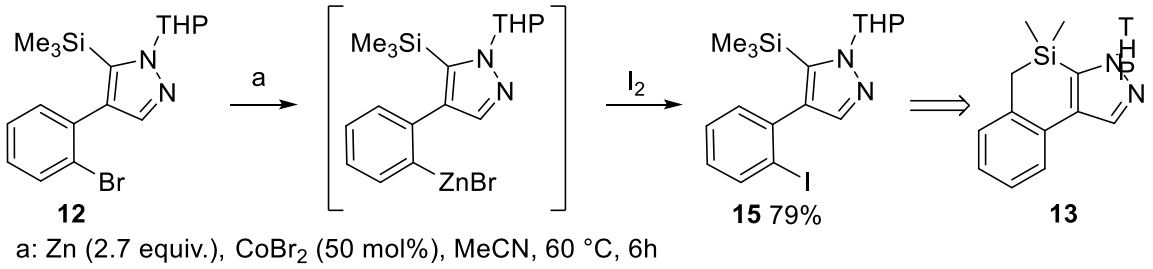

Scheme 11. Arylzinc route to isomer **15**.

An extensive optimization of the Pd-catalyzed C–H activation conditions led, almost quantitatively, to the expected tricyclic product **17**, the structure of which could be confirmed by X-Ray diffraction analysis. The deprotection of the pyrazole ring could be easily achieved using classical acidic condition to remove the THP group (Scheme 12). Note that the best cyclization conditions involved 5 mol % $Pd(OAc)_2$ and 10 mol % PCy_3 as a ligand, in the presence of 30 mol % PivOH and 2 equiv Cs_2CO_3 as base, in xylenes at 135 °C for 1 h. These conditions, which differ markedly from those reported by Xi,[22] suggested that the mechanism does not involve a proton abstraction, but, instead, proceeds via a fully concerted pathway involving a palladium carboxylate.

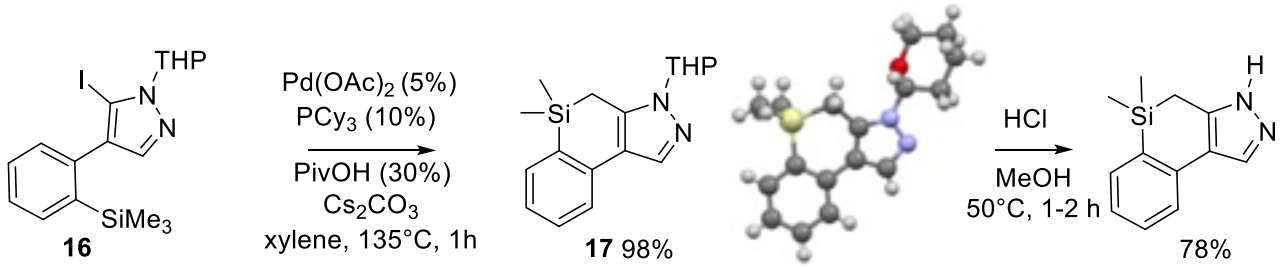

Scheme 12. Cyclization of **16** into benzosilinopyrazole **17** by Pd-catalyzed C–H activation.

This reaction sequence could be successfully extended to arylboronic acids bearing OMe or CF_3 substituents, provided that the reaction time was appropriately adjusted (Scheme 13). When treated in similar conditions, isomer **15** led also to the expected tricyclic product **13** in total conversion after 22h. Unfortunately, the limited chemical stability of **13** headed to relatively modest chemical yields of 32%.

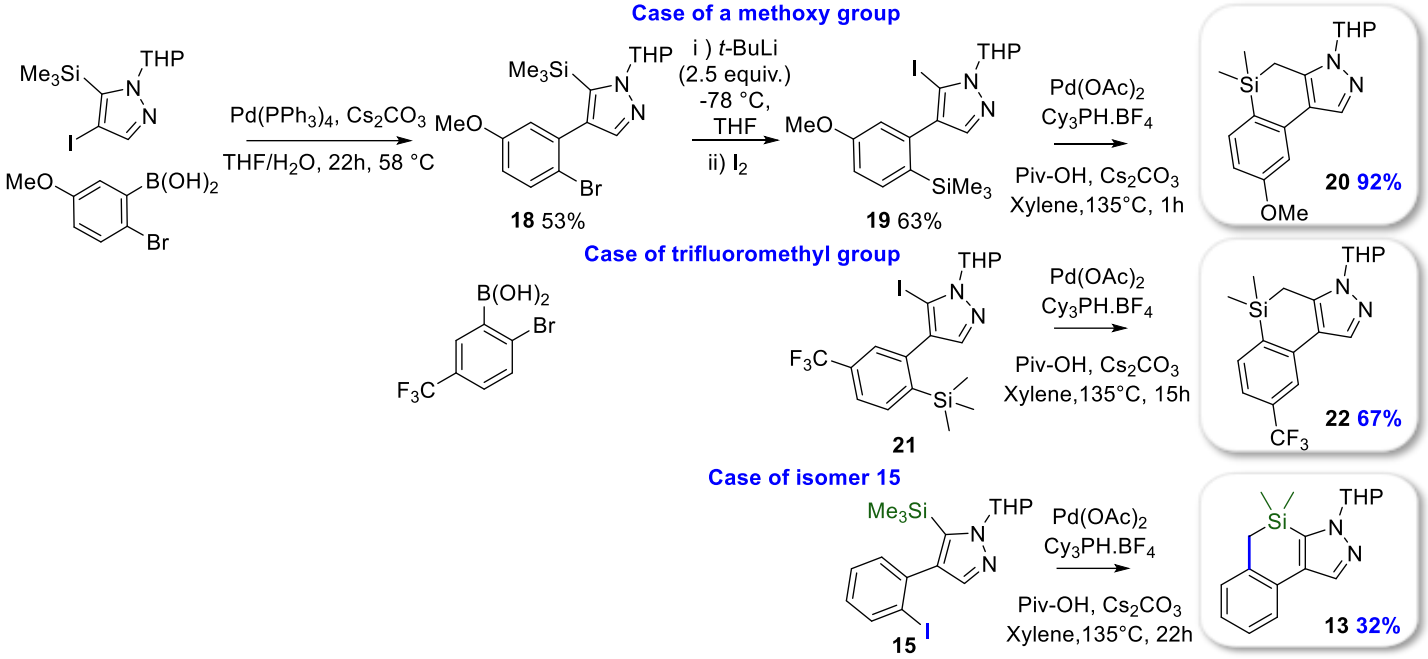

Scheme 13. Extension of the Pd-catalyzed C–H activation to benzosilinopyrazoles.

2.3. Synthesis of silylated heterocycle by silapalladation of alkynes and alkenes

Inspired by our previous work on the carbolithiation reaction,[26] we sought to explore the direct silametallation of alkynes as a route to silaheterocycles. This transformation would generate an exocyclic vinyl-metal intermediate, which could be further functionalized to give access a wide variety of target molecules (Scheme 14). The strategy was initially tested using disilane substrate **23**, readily prepared from *o*-iodophenol. However, treatment of **23** with alkali derivatives, following approaches reported by Buncel[27] or Hevesi,[28] resulted in complex mixtures or decomposition.

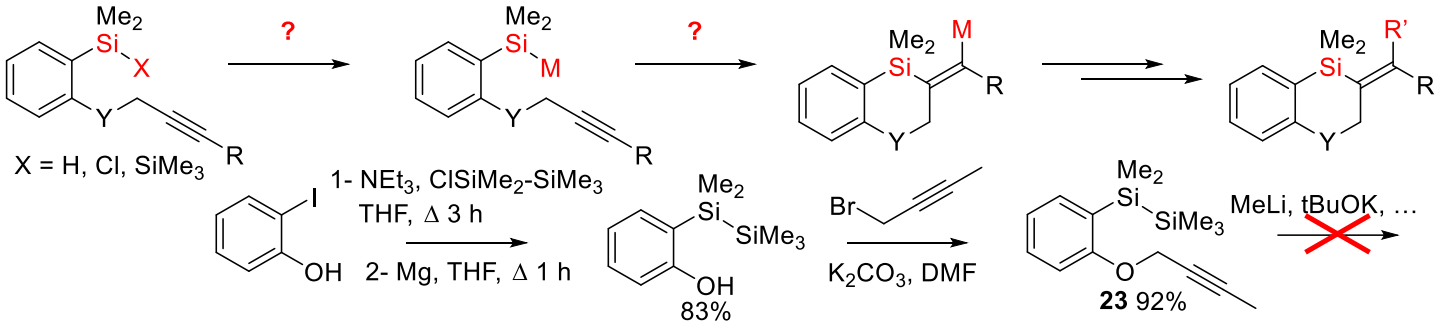

Scheme 14. Proposed access to silaheterocycles by direct silametallation.

We, therefore, retained the palladium-catalysis methodology developed by Sakurai for cyclic disilanes.[29] Following optimization, we achieved semi-quantitative cyclization, enabling the efficient, and fully stereo-controlled formation of 6-, 5-, and 4-membered silyl-heterocycles. The reaction proceeds via a *syn exo-dig* pathway, with both silicon atoms adding cleanly across the C–C triple bond, demonstrating both the generality and precision of this strategy (Scheme 15).[30]

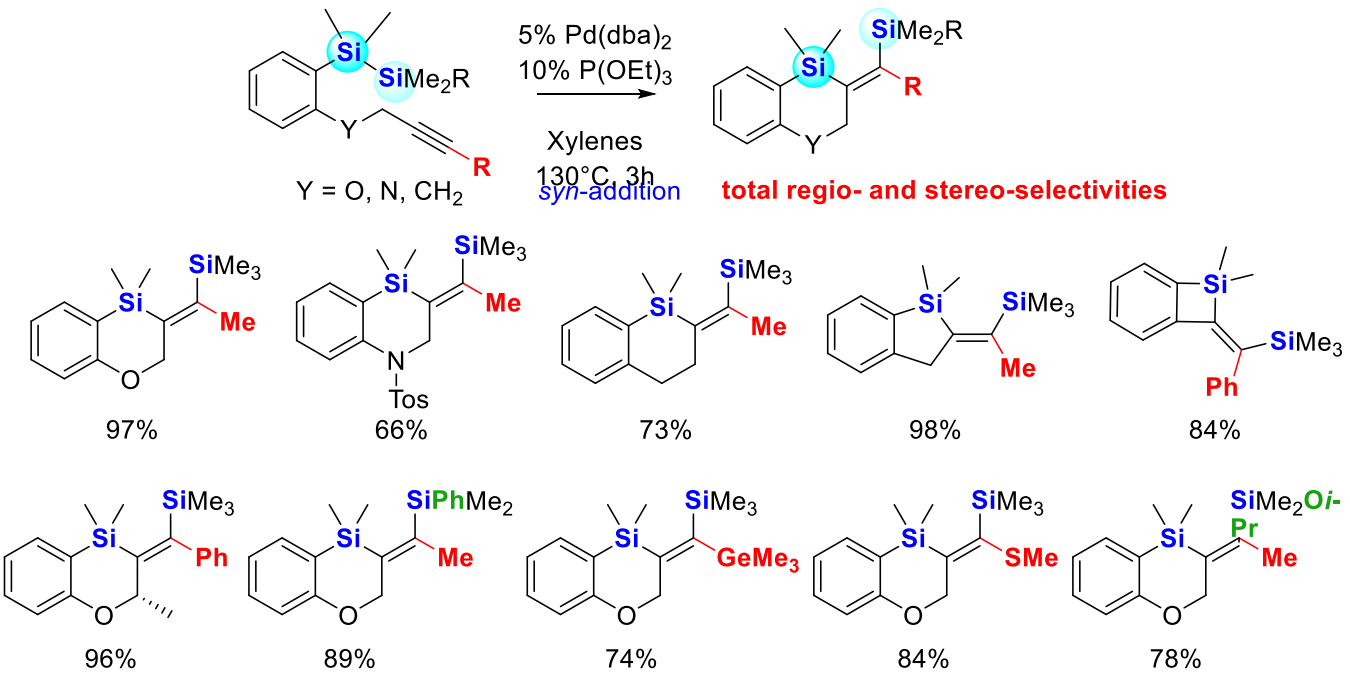

Scheme 15. Representative examples for the intramolecular silyl-palladation of alkynes.

This sequence proved to be highly general, accommodating triple bonds substituted with alkyl or aryl groups, and heteroatoms. It could even be extended to the synthesis of gem bis-heteroalkenes (SiSi, SiGe, SiS) as well as a variety of differently Si-substituted sila-alkenes. The connection between the aryl group and the triple bond could be O, N or C, and its lengths adjusted to enable the synthesis of 4- 5- or 6- member rings. Additionally, the substitution of the terminal silicon was successfully modulated. Notably, a $SiMe_2O$*i*-Pr silyl-ether could be employed, which was converted into the corresponding silanol upon hydrolysis. We took advantage of this latter reaction by performing an oxa-Heck reaction efficiently using activated olefins and Rhodium catalysis (Scheme 16). Surprisingly, when using ethylvinylketone, the reaction derailed toward an oxa-Michael process, leading to saturated silyl ethers. Finally, this divergent reaction could be generalized to other activated olefins simply by adding water to the solvent.

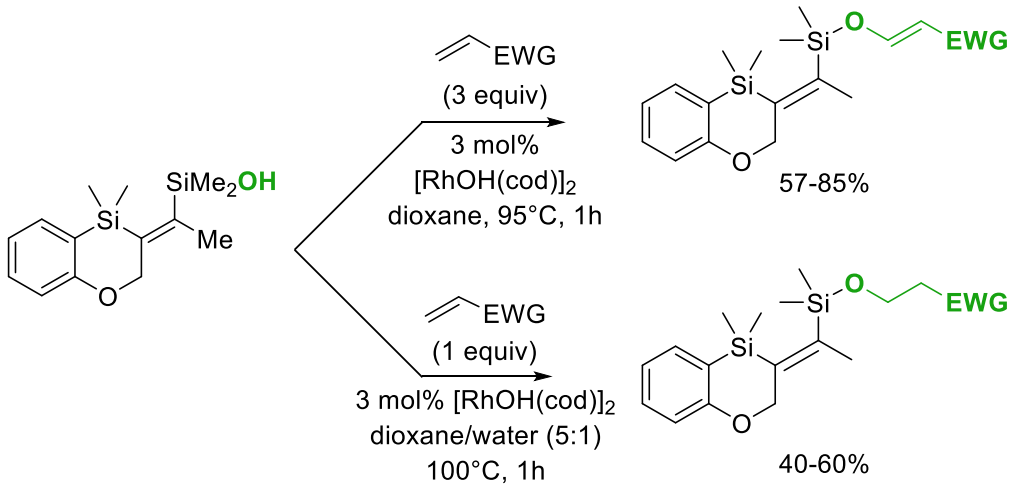

Scheme 16. Rhodium-catalyzed oxa-Heck and oxa-Michael reaction with silanol.

The extension of this reactivity to heterocyclic disilane scaffolds was subsequently investigated.[31] This study was initiated with pyridinic or quinolinic substrates, which are derived from starting materials prepared *via* a Li–Br exchange using *n*-butyllithium in the presence of chloropentadisilane at -95°C. Under the previously established conditions for the silyi-palladation conditions, the expected N-heterocycles-fused azasilines were obtained in good-to-excellent yields, while maintaining the same regio- and stereoselectivities (*syn exo-dig* addition, Table 2).

Table 2. Silapalladation of disilapyridine or quinoline

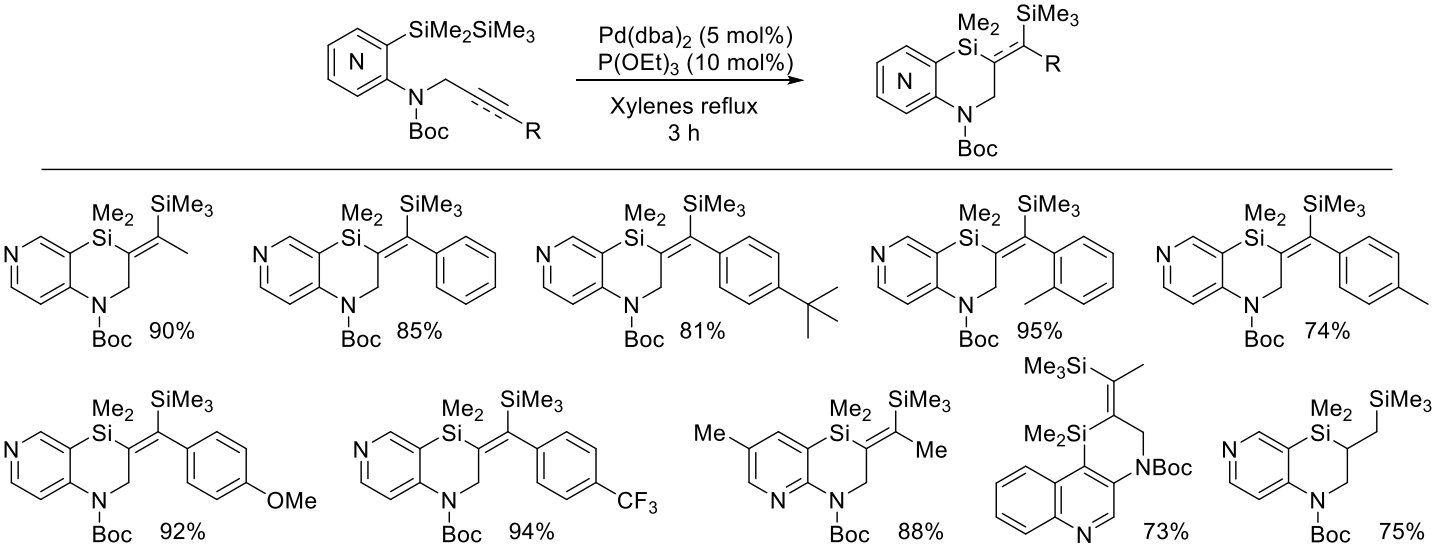

This methodology could be extended even further to the synthesis of structures incorporating phenothiazine, indole, carbazole or tetrahydroquinoline moieties. In order to access the corresponding precursors, adaptations of the two key steps—namely the introduction of the alkyne and the di-silane appendages—were required for each substrate family (Scheme 17).

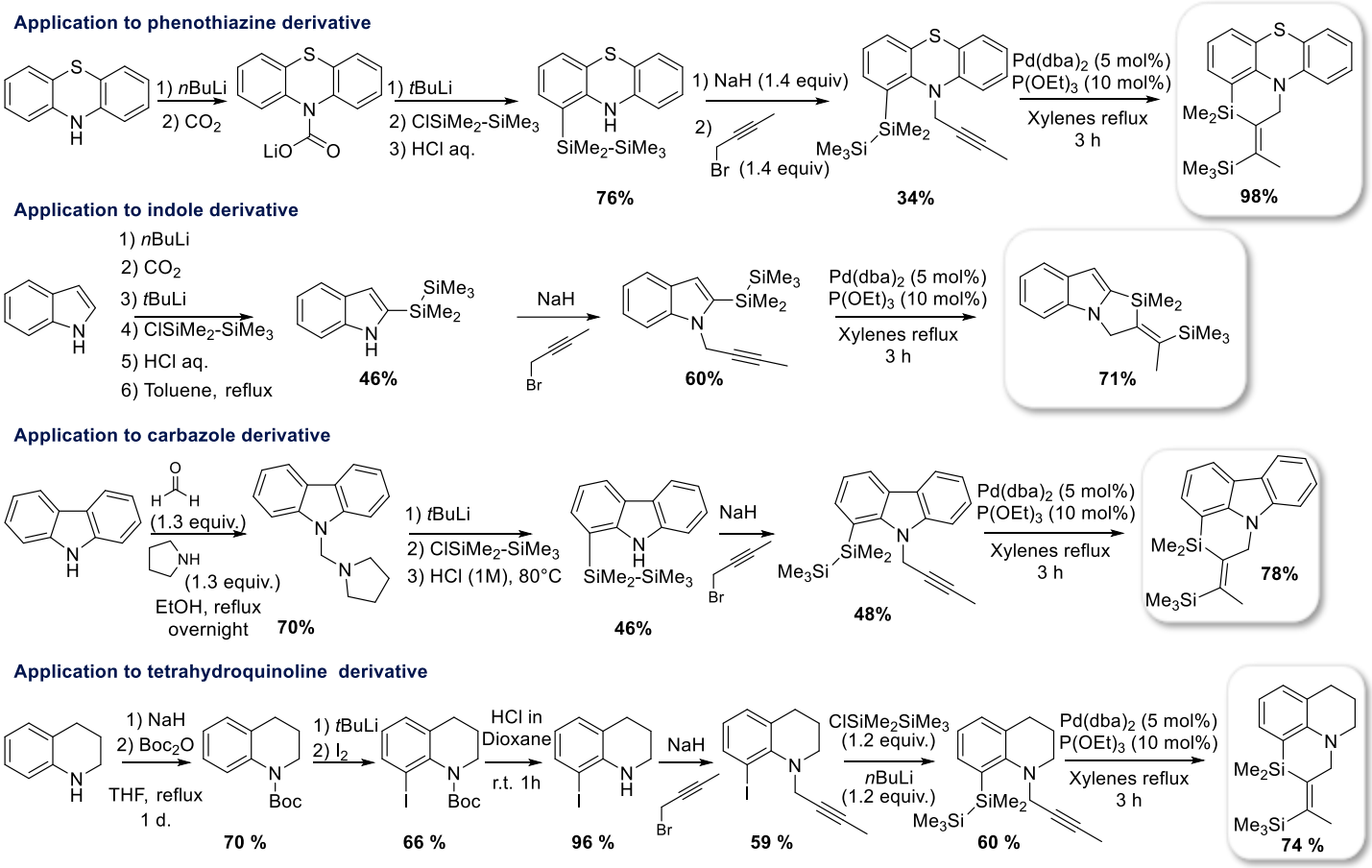

Scheme 17. Synthesis and silyl-palladation of phenothiazine, indole, carbazole or tetrahydroquinoline derivatives.

2.4. Synthesis of germylated heterocycles by Ge–H activation

As the silylmetallation strategy proved unsuccessful with disilanes, we turned to the well-established activation of Si–H or Ge–H bonds using non-noble metals such as Zn. This approach offers the additional advantage of providing access to vinylzinc intermediates, which can be further functionalized readily.

2.4.1. Synthesis of (benzo)germols by radical germylzincation. This strategy was first applied to the synthesis of germols and benzogermols.[32] Access to the starting materials required slight modifications to the procedure described above. The alkyne moiety was introduced via a Sonogashira coupling, followed by lithium-halogen exchange and subsequent addition of dichlorodiphenylgermane, then reduction of the remaining Ge–Cl bond. Upon addition of 1.5 equivalents of diethylzinc, cyclisation proceeded through a radical mechanism, and required the presence of 15 mol % of AIBN. The reaction exhibited a broad scope, as substitution at the triple bond or on the aromatic ring could be extensively varied (Scheme 18).

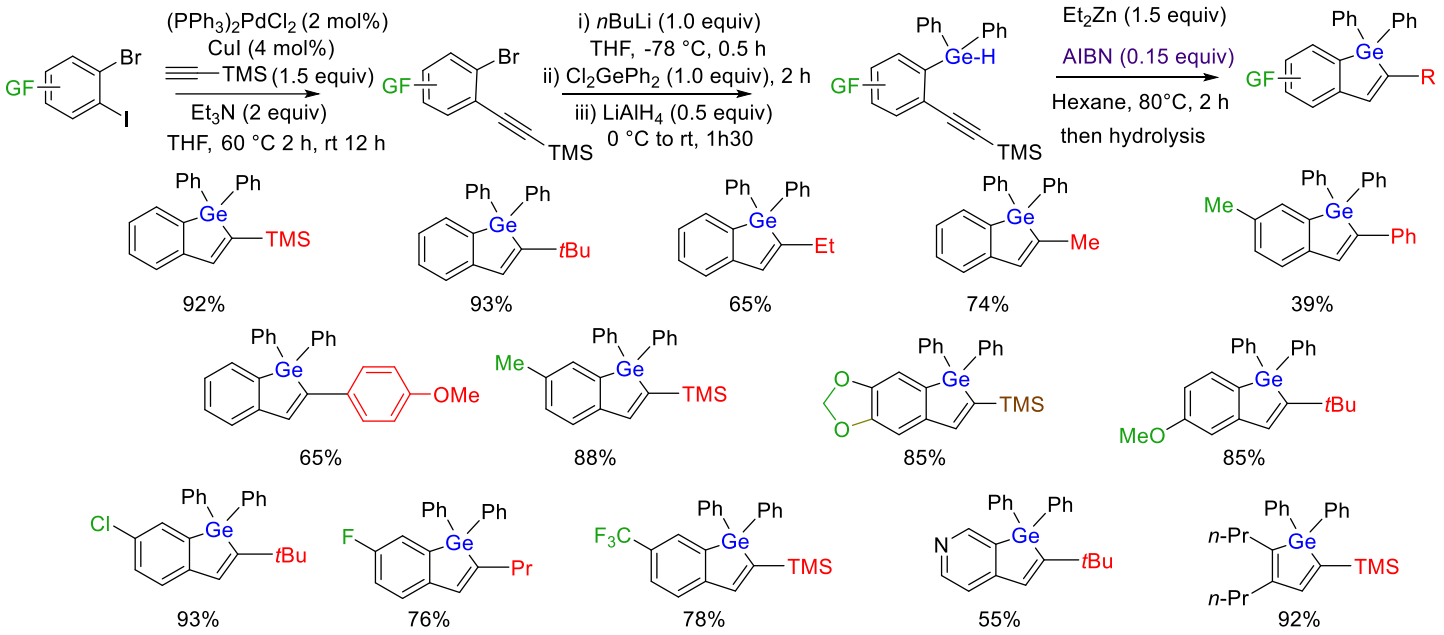

Scheme 18. Synthesis and intramolecular radical germylzincation.

The formation of an arylzinc intermediate was demonstrated by a deuteration experiment, which afforded the expected 3-deuterogermol in very good yield. We, therefore, decided to exploit this transient species through post-functionalization with various electrophiles in the presence of a copper catalyst (Table 3). Among those transformations, iodination deserves particular attention, as the resulting 3-iodogermol can be further converted *via* palladium-catalyzed reactions to afford new 3-aryl substituted derivatives.

Table 3. Functionalization of the germylzinc intermediate

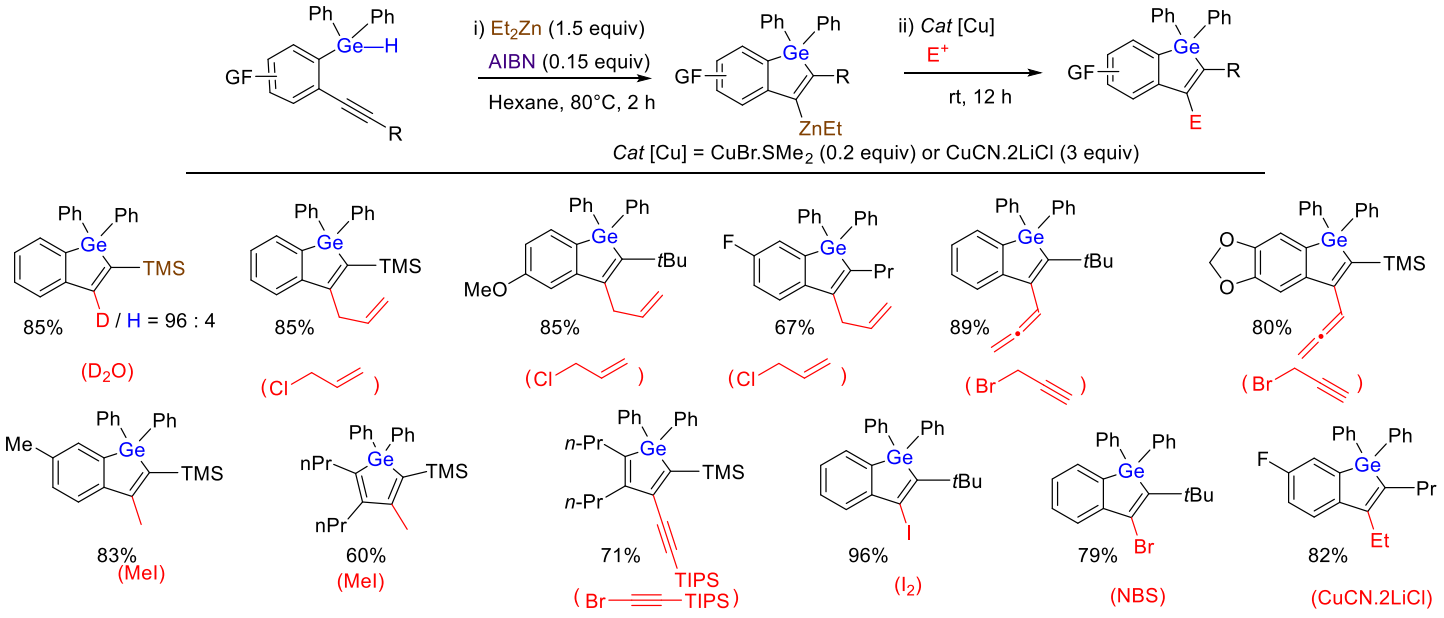

Mechanistically, the radical nature of the cyclization step was readily demonstrated. In the absence of AIBN, the reaction of dialkylzinc proceeds directly at the germanium atom via a germylzinc intermediate **D**, which is unable to undergo cyclization (Scheme 19). In the presence of AIBN, homolytic Ge–H cleavage generates a reactive germyl radical intermediate **A**, which cyclizes through a 5-*endo-dig* process to form radical **B**. Finally, reaction with Et_2Zn furnishes the zinc intermediate **C**, releasing an ethyl radical and thus completing the catalytic cycle.

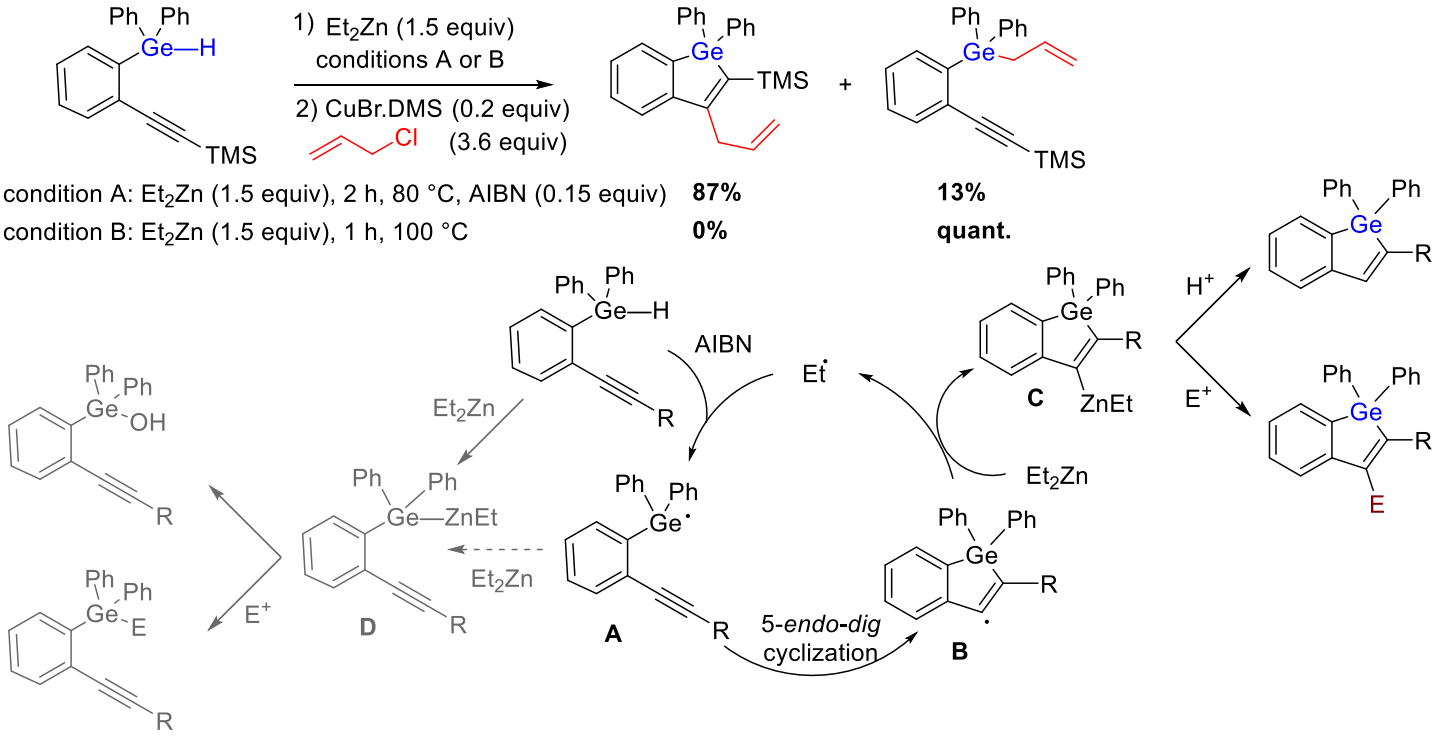

Scheme 19. Mechanistic investigation and proposed mechanism.

2.4.2. Synthesis of germylated heterocycles by polar germylzincation. To expand the reaction scope, we opted to shift the triple bond away from the aromatic ring, tethering it through an O–CH_2 moiety.[33] It should be noted that the preparation of these new substrates requires the use of Turbo-Grignard intermediates, rather than butyllithium, due to the competing carbolithiation of the triple bond. Under the radical germylzincation conditions described above, conversion remains quantitative, however, the stereoselectivity was found to switch from a major *syn* to a major *anti* selectivity, depending on the substrate (Table 4, entries 1-2). Performing the reaction with only one reagent (AIBN or R_2Zn) revealed two competing pathways: a purely radical pathway leading to the *anti*-product (with AIBN), and a purely polar one affording the *syn*-product (with *i*-Pr_2Zn) (Table 4).

Table 4. Optimization of the germylzincation

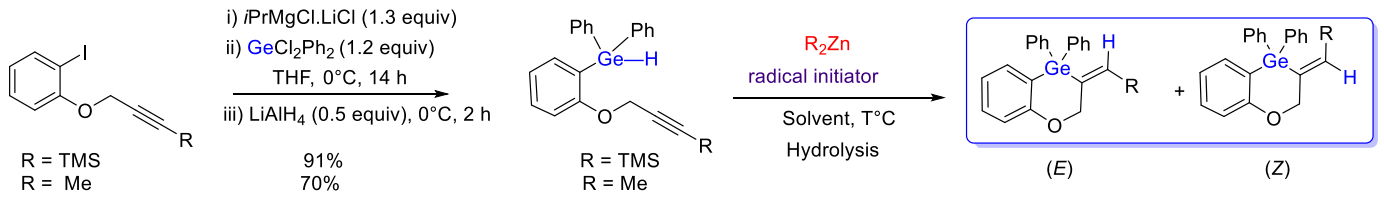

Entry	R	R_2Zn	Solvent	Conditions	Conversion	Ratio *E* / *Z* (*Syn* / *Anti*)
1	TMS	Et_2Zn (3 equiv)	Hexane	1 h, 100°C, AIBN (0.15 equiv)	100%	93 : 7
2	Me	Et_2Zn (3 equiv)	Hexane	1 h, 100°C, AIBN (0.15 equiv)	100%	15 : 85
3	TMS	Et_2Zn (3 equiv)	Hexane	3 h, 100°C,	92%	81 : 19
4	Me	Et_2Zn (3 equiv)	Hexane	3 h, 100°C,	71%	94 : 6
5	TMS	0 equiv	Hexane	1 h, 100°C, AIBN (0.15 equiv)	88%	3 : 97
6	Me	0 equiv	Hexane	1 h, 100°C, AIBN (0.15 equiv)	100%	0 : 100
7	TMS	iPr_2Zn (3 equiv)	Hexane[b]/Toluene : 3/1[c]	2 h, 100°C	100%	93 : 7
8	Me	iPr_2Zn (3 equiv)	Hexane[b]/Toluene : 3/1[c]	2 h, 100°C	100%	95 : 5
9	TMS	iPr_2Zn (1.2 equiv)	Hexane[b]/Toluene : 3/1[c]	1 h 30, 80°C	100%	94 : 6

The potential of the polar germylzincation has been demonstrated by applying this method to the synthesis of a dozen heterocycles, generally affording good yields and moderate-to-excellent stereoselectivities. Note that the *exo*-cyclic vinylzinc intermediate can be further exploited through direct trapping with various electrophiles (Table 5).

Table 5. Scope of the germylzincation and trapping of the zinc intermediate

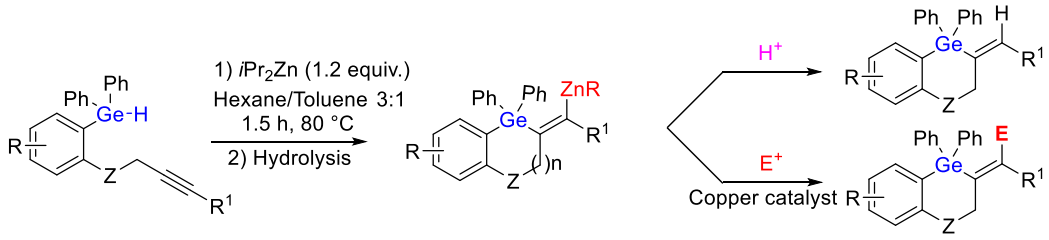

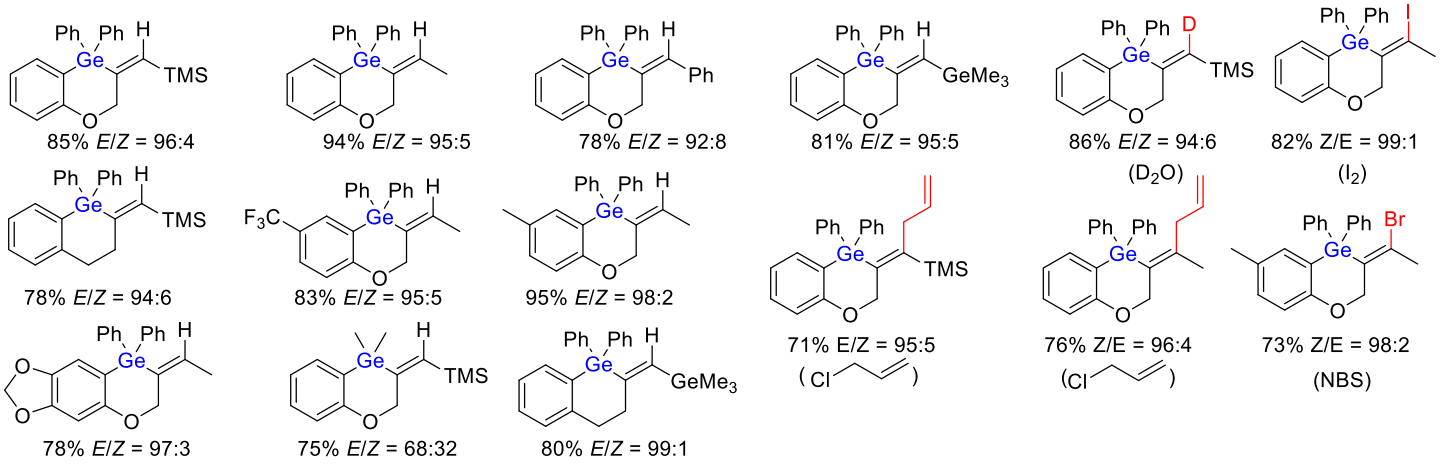

2.5. Synthesis of silylated heterocycles by Si–H activation

The direct extension of the above methodologies from Ge–H to Si–H proved to be ineffective. Hydrosilylation traditionally relies on a noble metal, particularly platinum, as catalysis.[34] A few examples describe iron, cobalt or nickel as efficient catalysts, mainly for the intermolecular version of this reaction.[35] Building on our expertise in nickel catalysis,[36] we were prompted to explore the possibility of an intramolecular nickel-catalyzed hydrosilylation. Initially, we generated the Ni(0) catalyst *in situ* by the conventional chemical reduction of Ni(II) salts with 2 equiv. of manganese metal in DMF at 50°C. In these conditions, the hydrosilylation of substrates **23** is efficient (40-100%) and regio- and stereoselective (following a *syn-exo-dig* process, Scheme 20). We found that the amount of manganese metal could be reduced to 0.26 equiv. without any impact on the yield of **24**,[37] suggesting that the reaction proceeds *via* a Ni(0) catalytic cycle.

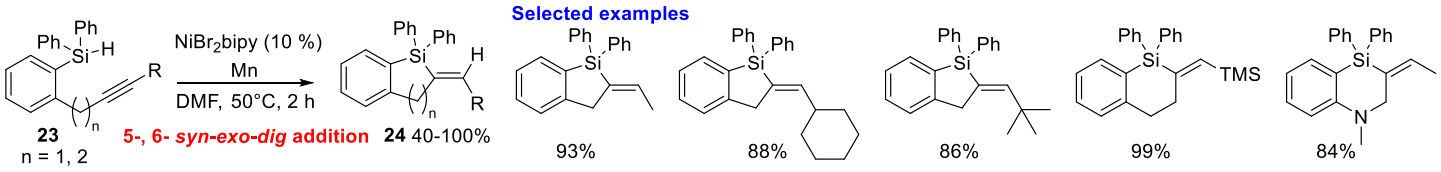

Scheme 20. Intramolecular Ni-catalyzed hydrosilylation.

We decided then to replace manganese by electrons and studied an electrochemical sacrificial anode process. The anode was either an aluminum or nickel plate, and the cathode is a nickel foam. Electrolysis was carried out most efficiently at 80°C under a constant current of 25-50 mA. It was not necessary to pass current throughout the entire process; 2F/mol of nickel salt (20 C, 5-10 minutes) was sufficient to generate Ni(0) *in situ*, after which the reaction mixture was stirred for 2 hours to achieve complete conversion of **23**. The scope of the process was evaluated under these conditions. This method is applicable to a variety of substrates and affords the expected silylated heterocycles **24** in good yields, in line with the high regio-and stereoselectivities observed above. Note that the $SiPh_2$ tether is more efficient than $SiMe_2$ (Table 6).

Table 6. Electrochemical intramolecular Ni-catalyzed hydrosilylation

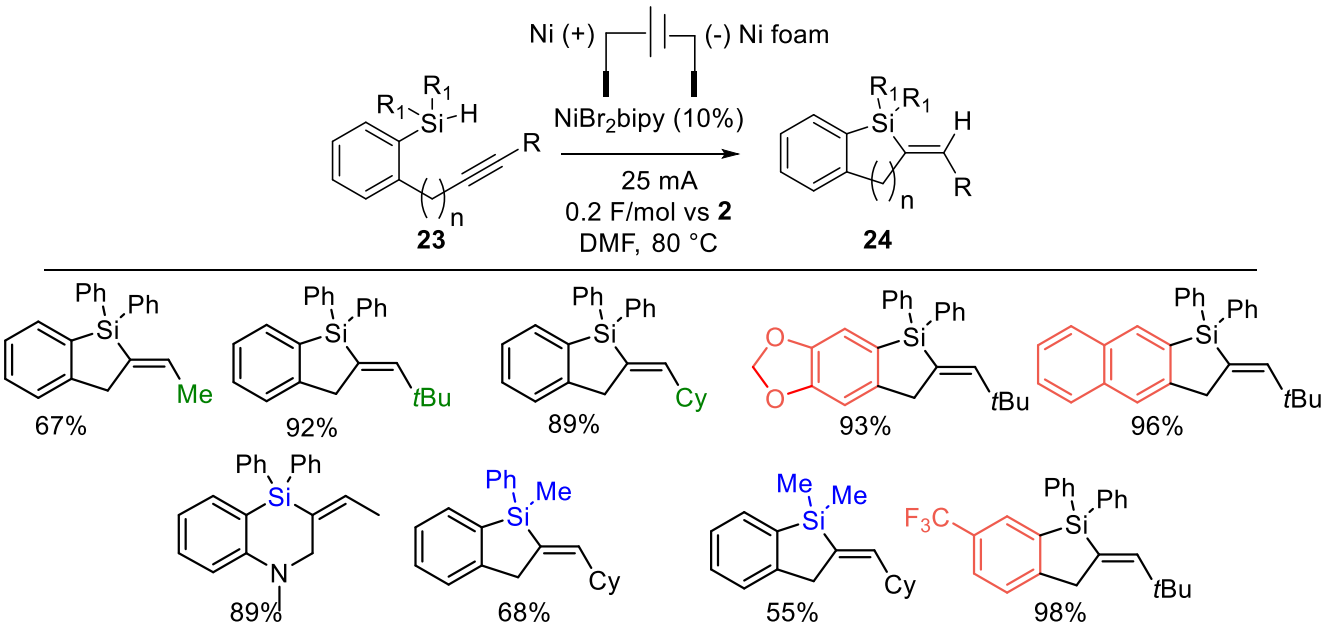

Interestingly, when the aryl moiety bears a bromine atom, Ni(0) can catalyze, in one-pot, the cyclization and cross-coupling reactions[38] (Scheme 21).

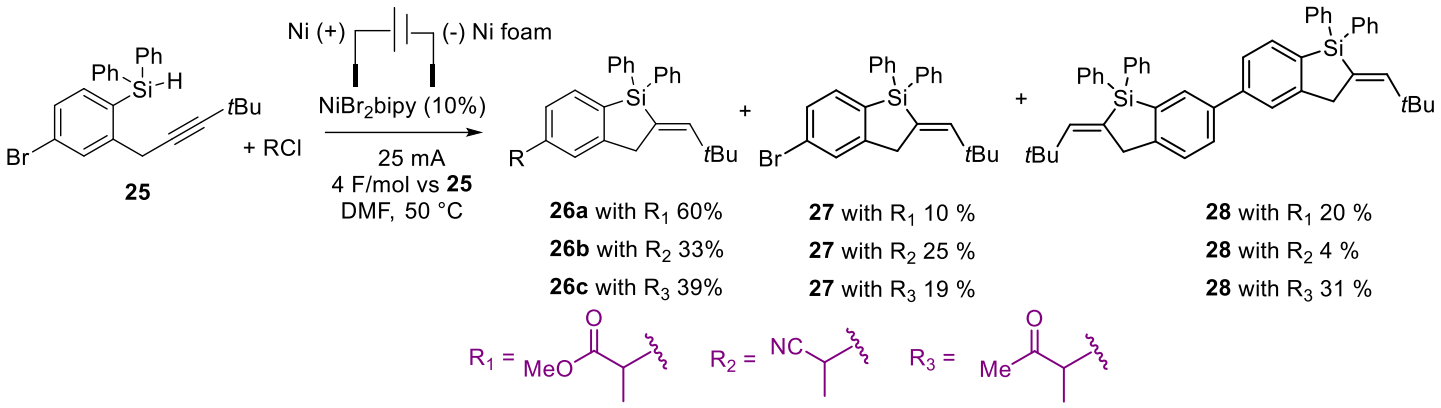

Scheme 21. Electrochemical nickel-catalyzed hydrosilylation/tandem cross-coupling reaction.

The mechanism was investigated by cyclic voltammetry, which enables us to propose the catalytic cycle depicted in scheme 22.

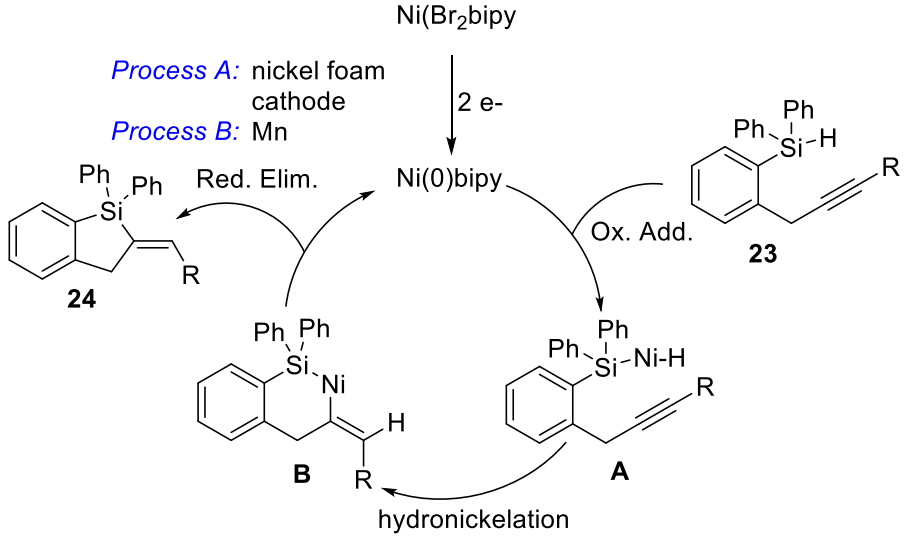

Scheme 22. Proposed mechanism for the nickel-catalyzed intramolecular hydrosilylation reaction.

The extension to alkenes was revealed to be easy, provided the temperature was adjusted to RT, and a terminal olefin was employed (Scheme 23).[39] Chemical yields are very high for both allyl- and vinyl-ether substrates, with perfect regioselectivity (*exo-trig* cyclisation). Once again, the yield decreased when diphenylsilane was replaced with its dimethyl analogue.

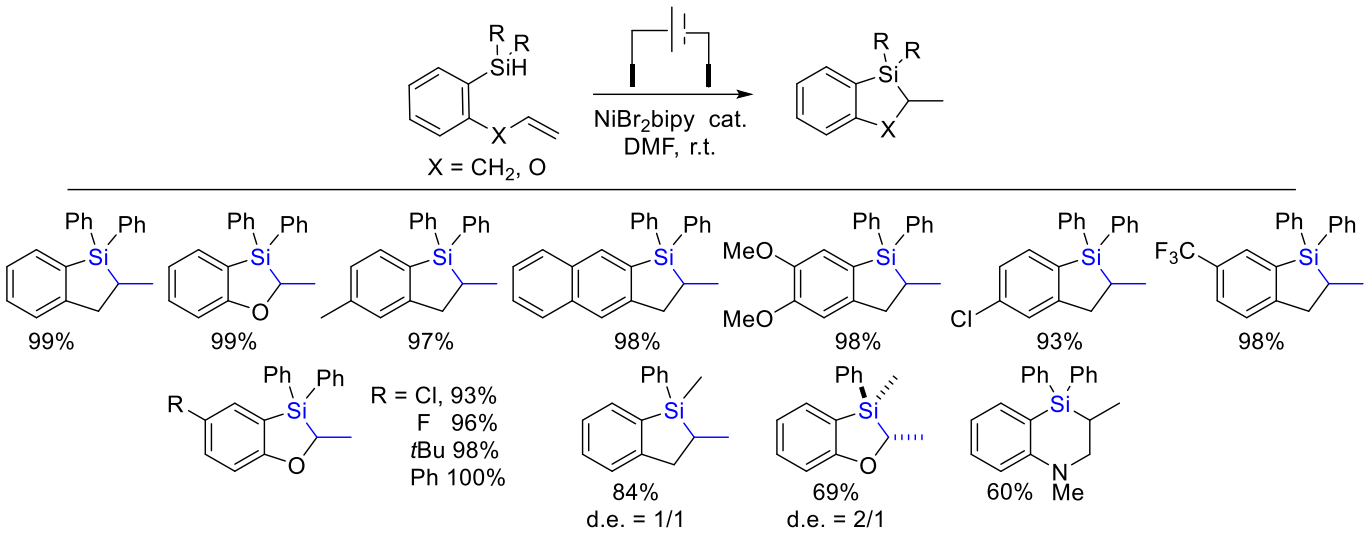

Scheme 23. Extension of the nickel-catalyzed intramolecular hydrosilylation reaction to alkenes.

Conclusions

In this account, we report various intramolecular strategies for the synthesis of fused 5- or 6- membered silylated and germylated heterocycles. These approaches are based on sila- or germylmetallation of double or triple C–C bonds, the hypervalent properties of silicon and germanium or on the C–H activation in α of the silicon. All methods employ non-noble metal catalysis, exhibit high regio and stereoselectivity, and provide the desired products in moderate-to-good yields. Given the relevance of such heterocycles in the pharmaceutical-chemistry, materials-sciences, and fragrances industries, these methodologies are expected to find broad utility. We anticipate that their versatility will allow adaptation to yet unexplored challenges.

Acknowledgements

We would like to sincerely thank all the (under)graduate students, with whom these reactions were explored and developed. Thanks also to our colleagues from Université de Rouen Normandie and CNRS for stimulating discussions. This work was partially supported by Normandie Université, the Région Normandie, the Centre National de la Recherche Scientifique (CNRS), Université de Rouen Normandie, INSA Rouen Normandie, Université Caen Normandie, ENSICAEN, Labex SynOrg (ANR-11-LABX-0029), the graduate school for research XL-Chem (ANR-18-EURE-0020 XL CHEM) and Innovation Chimie Carnot (I2C).

References

1. Berzelius, J. J. *Ann. Chim. Phys.* **1824**, *27*, 337–359.
2. Mills, J. S.; Showell, G. A. *Expert Opin. Invest. Drugs* **2004**, *13*, 1149–1157. https://doi:10.1517/13543784.13.9.1149
3. Showell, G. A.; Mills, J. S. *Drug Discovery Today* **2003**, *8*, 551–556.

https://doi:10.1016/s1359-6446(03)02726-0
4. Meanwell, N. A. *J. Med. Chem.* **2011**, 54, 2529–2591. https://doi:10.1021/jm1013693
5. Franz, A. K.; Wilson, S. O. *J. Med. Chem.* **2012**, *56*, 388–405. https://doi:10.1021/jm3010114
6. Petkowski, J. J.; Bains, W.; Seager, S. *Life.* **2020**, *10*, 84. https://doi:10.3390/life10060084
7. Panayides, J.-L.; Riley, D. L.; Hasenmaile, F.; van Otterlo, W. A. L. *RSC Med. Chem.* **2024**, *15*, 3286–3344. https://doi:10.1039/D4MD00169A
8. Tamao, K.; Uchida, M.; Izumizawa, T.; Furukawa, F.; Yamaguchi, S. *J. Am. Chem. Soc.*, **1996**, *118*, 11974–11975. https://doi:10.1021/ja962829c
9. Allard, N.; Badrou-Aich, R.; Gendron, D.; Boudreault, P-L.T.; Tessier, C.; Alem, S.; Tse, S. C.; Tao, Y.; Leclerc, M. *Macromolecules*, 2010, **43**, 2328–2333. https://doi:10.1021/ma9025866
10. Shimizu, M.; Hiyama, T. *Synlett* **2012**, 973–989. https://doi:10.1055/s-0031-1290566
11. Yabusaki, Y.; Ohshima, N.; Kondo, H.; Kusamoto, T.; Yamanoi, Y.; Nishihara, H. *Chem. Eur. J.*, 2010, **16**, 5581–5585. https://doi:10.1002/chem.200903408
12. Driess, M. Oestreich, M. *Chem. Eur. J.* **2014**, *20*, 9144-9145. https://doi: 10.1002/chem.201404080
13. Ramesh, R.; Reddy, D. S. *J. Med. Chem.* **2018**, *61*, 3779-3798. https://doi:10.1021/acs.jmedchem.7b00718
14. Hitchcock C. H. S., Mann F. G., Vanterpool A., *J. Chem. Soc.,* **1957**, 4537-4546. https://doi:10.1039/JR9570004537
15. Aoyama, T.; Sato, Y.; Suzuki, T.; Shirai, H., *J. Organomet.,* **1978**, *153*, 193-207. https://doi.org/10.1016/S0022-328X(00)85042-1
16. François, C.; Boddaert, T.; Durandetti, M.; Querolle, O.; Van Hijfte, L.; Meerpoel, L.; Angibaud, P.; Maddaluno, J., *Org. Lett.,* **2012**, *14*, 2074-2077. https://pubs.acs.org/doi/10.1021/ol300598s
17. Boddaert, T.; François, C.; Mistico, L.; Querolle, O.; Meerpoel, L.; Angibaud, P.; Durandetti, M.; Maddaluno, J, *Chem. Eur. J.,* **2014**, *20*, 10131-10139. https://chemistry-europe.onlinelibrary.wiley.com/doi/10.1002/chem.201402597
18. Hansch, C.; Leo, A.; Taft, R. W., *Chem. Rev.,* **1991**, *91*, 165-195. https://pubs.acs.org/doi/10.1021/cr00002a004
19. Boddaert, T.; Querolle, O.; Meerpoel, L.; Angibaud, P.; Maddaluno, J.; Durandetti, M., *Heterocycles*, **2018**, *97*, 1210. https://doi.org/10.3987/com-18-s(t)70
20. Sorbera, L. A.; Serradell, N.; Bolos, J.; Bayes, M., *Drug Future*, **2006**, *31*, 847-853. 10.1358/dof.2006.031.10.1040032
21. Khloya, P.; Ceruso, M.; Ram, S.; Supuran, C. T.; Sharma, P. K., *Bioorg. Med. Chem. Lett.* **2015**, *25*, 3208-3212.

https://www.sciencedirect.com/science/article/pii/S0960894X1500579X?via%3Dihub
22. Liang, Y.; Geng, W.; Wei, J.; Ouyang, K., Xi, Z., *Org. Biomol. Chem.* **2012**, *10*, 1537-1542. https://pubs.rsc.org/en/content/articlelanding/2012/ob/c2ob06941e
23. Mistico, L.; Querolle, O.; Meerpoel, L.; Angibaud, P.; Durandetti, M.; Maddaluno, J., *Chem. Eur. J*., **2016**, *22*, 9687-9692. https://chemistry-europe.onlinelibrary.wiley.com/doi/10.1002/chem.201601533
24. Fillon, H.; Gosmini, C.; Périchon, J., *J. Am. Chem. Soc.* **2003**, *125*, 3867-3870. https://pubs.acs.org/doi/10.1021/ja0289494
25. Begouin, J.-M.; Gosmini, C., *J. Org. Chem.* **2009**, *74*, 3221-3224. https://pubs.acs.org/doi/10.1021/jo900240d
26. Maddaluno, J.; Fressigné, C.; Durandetti, M., *Synlett* **2026**, *ASAP*. https://www.thieme-connect.com/products/ejournals/abstract/10.1055/a-2733-1807
27. Buncel, E.; Venkatachalam U.; Edlund, T. K., *J. Organomet. Chem.* **1992**, *437*, 85-89. https://www.sciencedirect.com/science/article/pii/0022328X9283433I
28. Hevesi, L.; Dehon, M.; Crutzen, R.; Lazarescu-Grigore, A., *J. Org. Chem.* **1997**, *62*, 2011-2017. https://pubs.acs.org/doi/10.1021/jo961131e
29. Sakurai H., Kamiyama Y., Nakadaira Y., *J. Am. Chem. Soc.*, **1975**, 97, 931-932. https://pubs.acs.org/doi/10.1021/ja00837a061
30. Ahmad, M.; Gaumont, A.-C.; Durandetti, M.; Maddaluno, J., *Angew. Chem. Int. Ed.,* **2017**, *56*, 2464-2468. https://onlinelibrary.wiley.com/doi/full/10.1002/anie.201611719
31. Noël-Duchesneau, L.; Maddaluno, J.; Durandetti., M., *ChemCatChem,* **2019**, *11*, 4154-4160. https://chemistry-europe.onlinelibrary.wiley.com/doi/10.1002/cctc.201900609
32. Kassamba, S.; Perez-Luna, A.; Ferreira, F.; Durandetti, M., *Chem. Commun.,* **2022**, *58*, 3901-3904. https://pubs.rsc.org/en/content/articlelanding/2022/cc/d1cc07163g
33. Kassamba, S.; Reboli, M.; Perez-Luna, A.; Ferreira, F.; Durandetti, M., *Org. Chem. Front*., **2023**, *10*, 3328-3335. https://pubs.rsc.org/en/content/articlelanding/2023/qo/d3qo00647f
34. Reboli, M.; Durandetti, M., *ChemCatChem.* **2025**, e202402136. https://chemistry-europe.onlinelibrary.wiley.com/doi/full/10.1002/cctc.202402136
35. Duarte de Almeida, L.; Wang, H.; Junge, K.; Cui, X.; Beller, M., *Angew. Chem. Int. Ed.*, **2021**, *60*, 550-565. https://onlinelibrary.wiley.com/doi/10.1002/anie.202008729
36. Durandetti, M., *Chem. Rec.*, **2021**, *21*, 3746-3757. https://onlinelibrary.wiley.com/doi/full/10.1002/tcr.202100142
37. Reboli, M.; Kassamba, S.; Durandetti, M., *Chem. Eur. J.*, **2024**, *30*, e202400440. https://chemistry-europe.onlinelibrary.wiley.com/doi/full/10.1002/chem.202400440
38. Durandetti, M.; Nédélec, J.-Y.; Périchon, J., *J. Org. Chem.*, **1996**, *61*, 1748-1755. https://pubs.acs.org/doi/10.1021/jo9518314
39. Reboli, M.; Durandetti, M., *ACS Omega*, **2026**, *11*, 10807-108013. https://pubs.acs.org/doi/10.1021/acsomega.5c13201

Authors' Biographies

Muriel Durandetti, born in 1968 in Saint-Etienne, France, is a Professor at the Rouen Normandie University. She completed her PhD, under the supervision of Professor Jacques Périchon on nickel-catalyzed electrosynthesis, in 1994 at University of Paris VI. She then worked for 4 years as an assistant professor at the University of Paris XII. In 1998, she obtained an associate professorship and developed electro-catalyzed cross-coupling reactions using nickel, chromium or iron salts. She complemented this work with mechanistic studies using electroanalytical processes. In 2005, she joined Rouen University as Associate Professor, and was promoted full Professor in 2023. Her research interests focus on electrosynthesis, intramolecular cyclization reaction by carbo- or hetero-metallation, or the synthesis of silylated heterocycles, opening up new strategies for generating valuable scaffolds.

Jacques Maddaluno, born in 1958 in Philippeville (Algeria), is a CNRS research fellow since 1989. He obtained his PhD in organic chemistry in ESPCI Paris in 1986, under the supervision of Dr Jean d'Angelo. He then joined Stanford University Medical School in Dr Kym Faull and Prof. Jack D. Barchas team to study ^{15}O-labelled L-DOPA. Hired by CNRS, he returned to France in 1989 and joined Prof. Pierre and Dr Lucette Duhamel's laboratory in University of Rouen where he focused on chiral lithium amides in asymmetric synthesis. He also collaborated with Dr Claude Giessner then Prof. Hélène Gérard (Sorbonne Université) in theoretical chemistry, and with Prof.

Hassan Oulyadi (University of Rouen) in NMR spectroscopy. After working at CNRS headquarters for 14 years, he moved in June 2025 to the Laboratoire d'Archéologie Moléculaire et Structurale in Paris.